# Analysis of Lift Forces on Fin Foils
# OCE 311 Final Report

Jackson Compton
Nick Grum
Tristram Howard
Ethan Koproski
Cecilia Schneider

May 10, 2019

# Contents



# List of Figures



# List of Tables

# 1 Abstract

This experiment was undertaken with the purpose of determining the lift coefficients of the steering fins on the Bluefin Sandshark autonomous underwater vehicle (AUV) for varying angles of attack. The objective was accomplished by creating an apparatus which measured the lift forces generated by the fin in a flow-tank or flume at differing angles of attack, and then solving the lift-force equation for the lift coefficients at those angles. The lift coefficient was plotted as a function of angle of attack and was observed to increase with the angle of attack up to around 15 degrees before stalling. Further testing, a faster flow channel, and a more accurate method of measuring the angle of attack would have been beneficial to the experiment.

# 2 Introduction

The Bluefin SandShark is autonomous underwater vehicle designed by Bluefin Robotics, as part of General Dynamics Mission Systems. It was designed for use by the United States Navy but it also can be used for a variety of various applications. For the Navy, the SandShark can perform several military missions including anti-submarine warfare, mine counter measurements, port and harbor security, and mobile acoustic countermeasure and decoy. Besides military purposes, the SandShark can also be used for offshore oil and gas pipeline inspections, shipyard maintenance, seafloor mapping, littoral surveys, and general environmental and oceanographic research.


Figure 1: Bluefin Sandshark

The system itself is relatively small and inexpensive when compared to other underwater vehicles. The SandShark is equipped with a customizable payload and can range between 74 and 111 centimeters in total length with a 12.4 centimeter diameter. All of the core vehicle systems including the lithium-ion battery pack and main system electronics are housed in the tail. The customizable payload allows for the attachment of several other systems including side scan sonars, depth sensors, GPS for surface use, acoustic sensors, inertial measurement units to track the motion of the AUV, and several others. The SandShark is rated to 200 meters depth and ranges in speeds between two and four knots. The fins, located on the tail just forward of the thruster, are an essential component that control the motion of the AUV. They provide active roll stabilization for the AUV as well as allow the AUV to ascend and descend in the water column. Horizontal fins control rising and diving motions while vertical fins control gyratory motion. The fins can also be interchanged onsite between smaller and

larger fins depending on intended operating speeds. Large fins are typically used at lower speeds while smaller fins are typically used at higher speeds.

The fins on the Bluefin SandShark are a type of hydrofoil. Fins are an essential component in minimizing energy consumption while still maintaining exceptional maneuverability. Similar to how the wings of an aircraft allow airplanes to fly, hydrofoils produce hydrodynamic forces that allow the AUV to move through the water. These hydrodynamic forces can be decomposed into two directions: lift and drag. Drag is the force produced parallel to the direction of flow. Lift is the force generated perpendicular to the direction of the flow and depends on the lift coefficient CL. The lift coefficient is given by:

$$C_L = \frac{F_L}{\frac{1}{2}\rho U^2 A} \tag{1}$$

Where $F_L$ is the lift force, $\rho$ is the fluid density, $U$ is the flow velocity, and $A$ is the planform area. The lift coefficient is determined experimentally from the measured lift force and can be plotted as a function of the angle of attack. The angle of attack is the angle between the foil and the incident fluid. This concept is illustrated below in Figure 2.

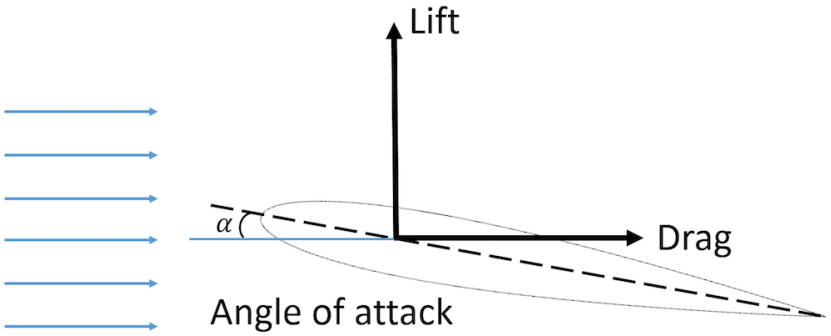


Figure 2: Illustration of lift, drag, and angle of attack.

As the angle of attack is increased, the magnitude of the lift coefficient will also increase. It will do do until it reaches a maximum angle of attack at which the foil will stall due to separation of the flow. An ideal plot of the lift coefficient versus the angle of attack is shown below in Figure 3.

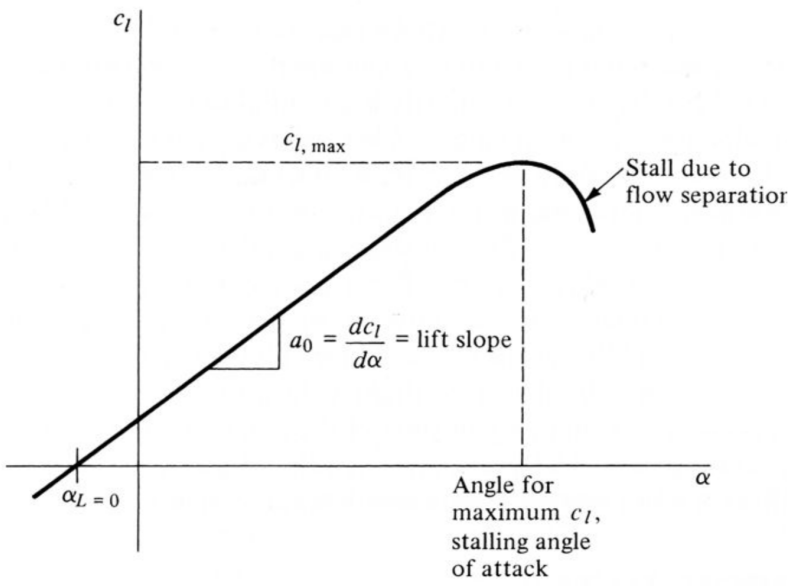


Anderson, J. D. (2016). *Introduction to flight*. New York, NY: McGraw Hill Education.

Figure 3: Theoretical plot of lift coefficient v.s. angle of attack.

The fins tested in this experiment are symmetric, which means that at an angle of attack of zero degrees, the lift coefficient would also be zero. It is expected that the resultant plot produced from experimental results would look similar to the plot in Figure 3, except shifted to the right to have an $x$ and $y$ intercept of zero.

# 3 Experimental Methods

In order to test the lift of the prototype fin first, a device needed to be invented to effectively carry out this task. To begin the design process, some basic fin lift research was conducted to get ideas for aspects that needed to be designed for. After a basic understanding of how fins create lift from a flowing media which in this case, was water, preliminary drawings were made. Going off of the idea provided by Stephen Licht, an adequate design was composed. Shown below in Figure 4 is the drawing of the device's initial design.

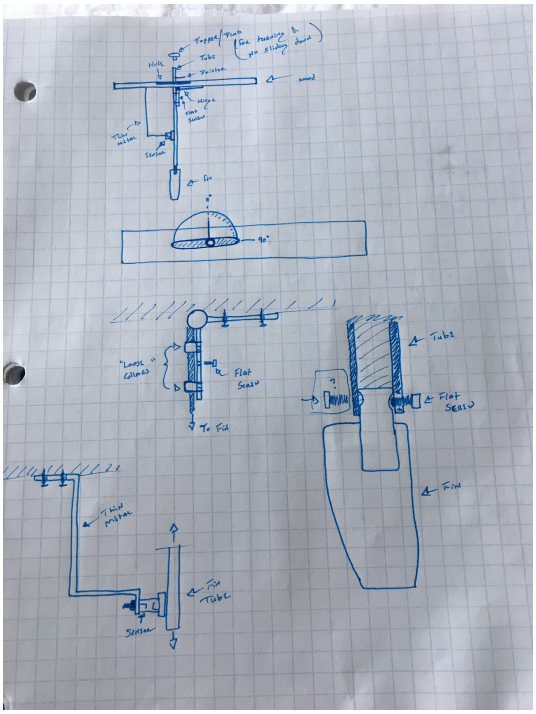


Figure 4: Preliminary apparatus design.

As shown above, the base of this device was originally supposed to be a thin plank of wood with a large elliptical hole cut out of the middle. Once in the shop, it was decided that a transparent rectangularly-cut piece of plastic was cut and used instead. This was done so that from the top-down view during testing, the ink vortices could be observed coming off of the fin's tail end. Additionally, the large elliptical hole was changed to a circular 0.5" hole as the post was not going to move that much during the testing. Although the hinge used was very smooth and loose, with the addition of the sensor, the post did not end up moving very much. The original hinge design can be seen below in Figure 5

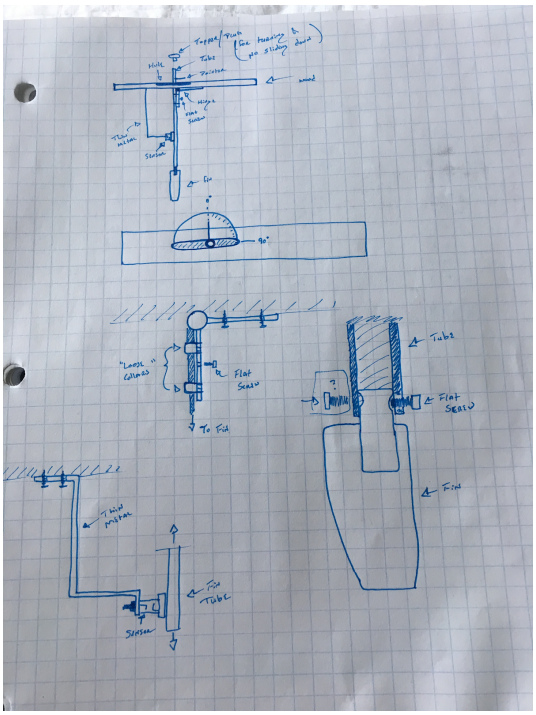


Figure 5: Hinge design.

As seen above, the initial design for the hinge system incorporated two collars as well as a small screw to hold the post in place after changing the angle. These proved more difficult to manufacture in the Middleton shop so instead, a worm screw clamp was found and used to hold the post in place. The post that was used for this device was a hollow metal pipe that was found in the Middleton shop. When it was found, there was a sealant or glue plugging one end of it however, it was drilled out and the fin ends fit snugly in that end. To ensure that the fin would not move during testing, a small 6-31 x 0.25" screw was put into the side and tightened when the fin pointed to zero degrees. Shown below is the original drawing for the fin keeping design.

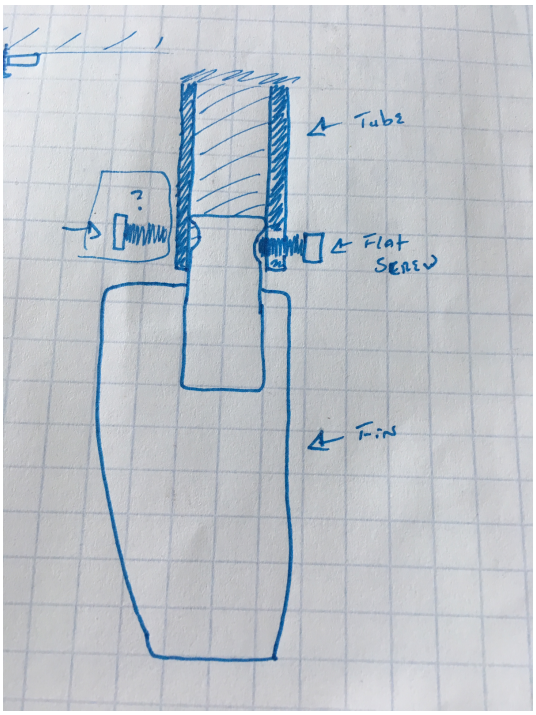


Figure 6: Fin attachment design.

With the hinge system attached to the base and the fin fixed to the post, the sensor was then needed to be fitted to the device. The original sensor holding system can be seen below however, this was changed during the manufacturing of the final design.

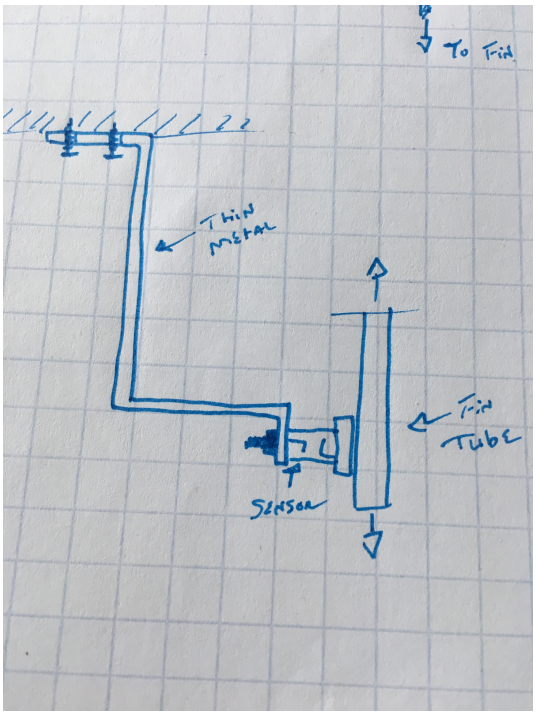


Figure 7: Force sensor attachment design.

Shown above, the original design for the sensor holding system was drawn to have a few angles in the thin metal strip to keep it out of the way. This was changed when better materials were found in the shop. To avoid having more than necessary calculations on the moment arm between the sensor and the base, the sensor apparatus was made straight instead. The sensor was attached to a small rectangular-cut piece of plastic from the same sheet as the base. This was again done to use the transparent properties of the plastic for observational purposes during testing and again to minimize the amount of moment arm calculations that needed to be done in order to find the appropriate lift force created by the fins. Attaching this to the base so that the sensor was just kissing the post was done using a green composite elbow that was found and cut to size in the Middleton shop. The final design is shown below in Figure 8.

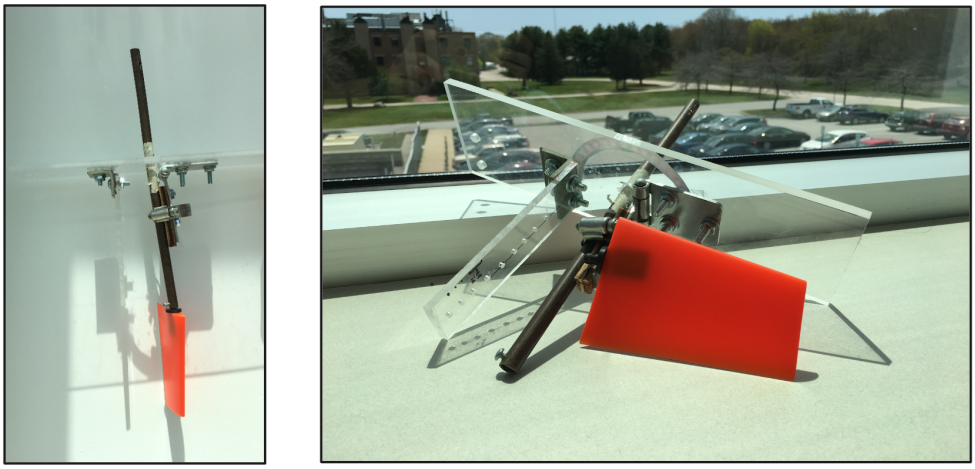

Figure 8: Final design of fin apparatus.

Once the device was constructed, it was time to bring it to the flow tank. Located in the lower level of the Watkins building of URI's Bay Campus, the flow tank needed to cleaned and filled. After this, the largest fin was fixed to the system in order to determine the maximum lift that these protype fins could generate. After adhering a protractor to the base of the device and having an added pointer to the post, the fin was set to its zero-degree position and the first test was run at 4.8 inches per second. With the sensor sending data to the computer, this test was saved and the next angle was set up. This same process was conducted for more angles as shown in the results section in order to find the critical angle of attack that would provide zero lift and the fin would stall. Some of the tests were conducted with a short expulsion of dye from the flow tanks dye system. This was done to show the vortices that trail off of the fin's tail end. After all of the data for the large fin was collected, the smallest fin that was provided was fixed to the post and some tests with the same methodology were conducted. Experimental setup is shown below in Figure 9.

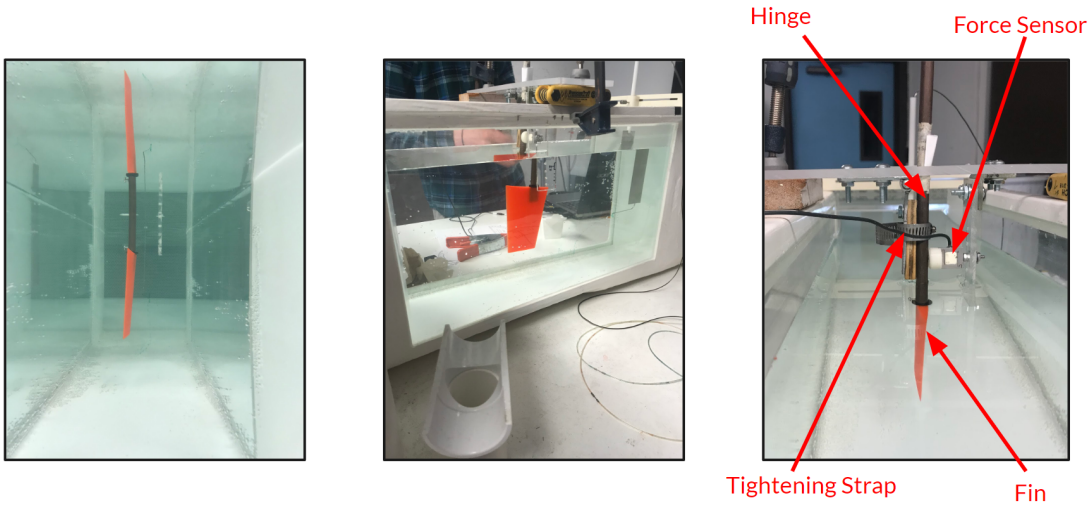


Figure 9: Experimental setup of fin apparatus in the Watkins Flow Tank.

Once all of the data was collected, it was converted to files which could be read on any computer. These were then read in MatLab to further analyze the findings. Using Equation 1, the lift coefficient for each fin was found. From this, the maximum effective angle of attack could be found by plotting in MatLab. In MatLab, plots were created to illustrate lift coefficient as a function of angle of attack and illustrate the point which the lift force stalls.

# 4 Results

After the force sensor measurements were converted to lift using moment arm calculations and then zeroed, the following plot was produced using Matlab (See Appendix):

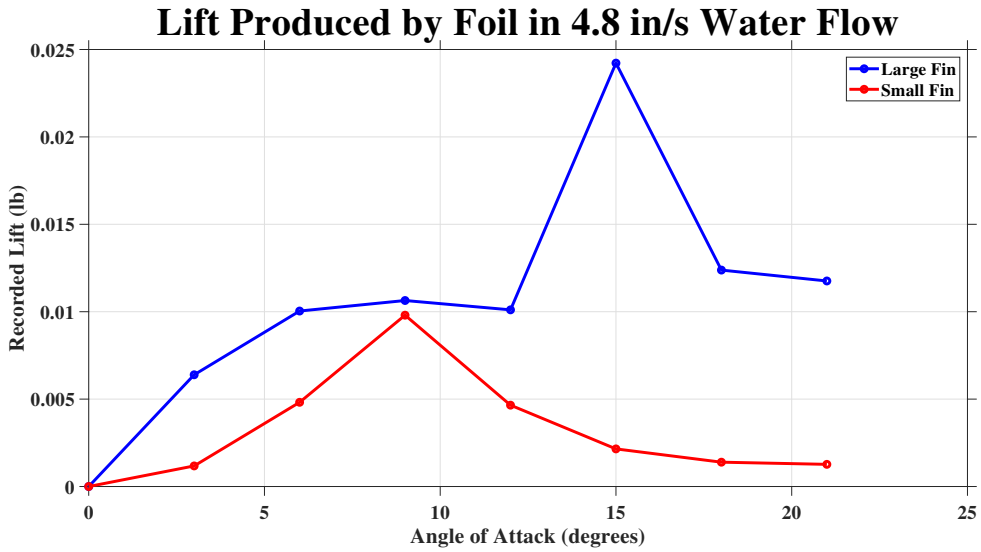


Figure 10: Lift as a Function of Angle of Attack for Differently Sized Foils in Freshwater

This figure plots the lift force in pounds against the angle of attack and illustrates where maximum lift is generated. Each point represents an averaged series of values recorded at the corresponding angle. The large fin produces overall greater lift than the small fin and both have different apparent peak angles. The small fin produces a maximum lift of about 0.01 lb at a 9 degree angle and the large fin produces a lift of close to 0.024 lb at a 15 degree angle of attack. This data was then used to convert to a plot of the lift coefficient as a function of the same angles of attack. In order to calculate the lift coefficient, however, some variables had to be defined. First, since the experiment was performed in freshwater, the fluid density was assumed to be:

$$\rho = 1000\text{kg/m}^3 \tag{2}$$

which is the acceptable value for freshwater. Next, the flow velocity was set to the maximum capability of the tank which provided:

$$U = 4.8\text{in/s} = 0.122\text{m/s} \tag{3}$$

The planform area of the fins also had to be measured and provided the following values for the large and small fins respectively:

$$A_{large} = 0.00657\text{m}^2 \tag{4}$$

$$A_{small} = 0.00269\text{m}^2 \tag{5}$$

With these known values, along with the lift forces at each angle, the following plot could be produced using a Matlab script (See Appendix):

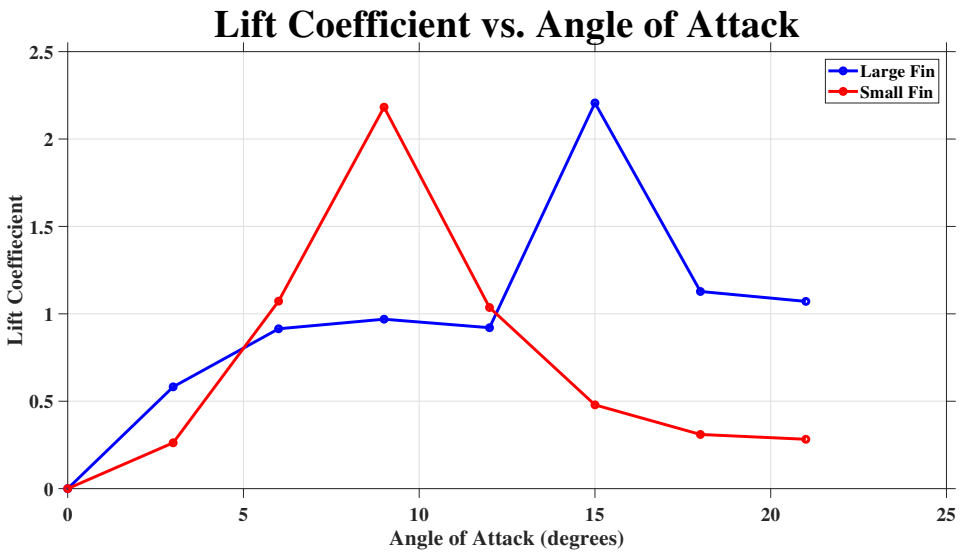


Figure 11: Lift Coefficient as a Function of Angle of Attack for Differently Sized Foils

The plot shows similarly shaped curves with peaks at the same angles. Both appear to have a maximum lift coefficient of around 2.25 at their respective angles. The table of values used to create these plots are included in the Appendices of this report.

# 5 Discussion

From the plots presented above with the lift force produced and the lift coefficient vs the angle of attack in Figures 10 and 11, it can be seen that the force sensor did not record a perfectly linear relationship but did seem to follow the expected pattern more or less. The lift increases as the angle of attack increase until a max lift is achieved and then begins to stall and lose forces of lift.

The large fin was seen to have the most non-linear changes as the angle of attack was changed. At approximately 15 degrees a maximum lift force was produced at around 0.024 lbs (0.11 Newtons) and had a lift coefficient of around 2.25. There was an outlier point with the large fin as the lift for the 12 degree angle of attack was smaller than the 9 degree angle of attack, which disagrees with the theory but could be attributed to possible measurement and equipment errors. The small fin had more linear changes, keeping a relatively straight line as the lift progressed through different angles. This fin achieved its maximum lift at 9 degrees with about 0.0095 lbs (0.042 Newtons) and a lift coefficient of around 2.25 as well based on inspection.

The testing environment in the Watkins flume tank was able to generate values of lift on the fins but the tank was maxed out at it's top flow rate of 4.8 inches per second, which translates to around a quarter of a knot. The Bluefin Sandshark AUV that operates with these fins generally travels in a 2-4 knot range. The team would want future tests to be conducted in faster moving water to generate more substantial force values and also see the responses of the fins in water velocities that they would commonly encounter while in operation.

It was noted in our presentation by Professor Dahl that the specific types of fins used on this AUV respond differently when attached close to a wall or surface, doubling their forces than when the fin is more or less isolated in the flow. A quick modification of the testing system with an added surface where the fin is situated would possibly improve the results and increase the validity of the experiment.

# 6 Conclusion

The production of an apparatus to measure lift forces generated by a fin was successful, as was its use. Also successful was the calculation of lift coefficients. This study neglected any effects that the nearby walls may have had on the measurements.

Were this experiment to be attempted again, it would be useful to devise a more accurate means of measuring the angle of attack; the paper protractor was determined to be somewhat inaccurate, especially after one occasion when it was dampened while adjusting the fin. It may also be advisable to use a flume which can attain speeds nearer those of the actual AUV, around 1 to 2 meters per second.

# References

Anderson, J. D. (2016). *Introduction to flight.* New York, NY: McGraw Hill Education.

General Dynamics. (2019). Bluefin SandShark Autonomous Underwater Vehicle (AUV) - General Dynamics Mission Systems. Retrieved from https://gdmissionsystems.com/en/products/underwater-vehicles/bluefin-sandshark-autonomous-underwater-vehicle

Hall, N. (2015, May 5). *NASA: Newton's Third Law Applied to Aerodynamics.* Retrieved from https://www.grc.nasa.gov/www/k-12/airplane/newton3.html

Licht, S. (2019). *Lift Force Notes* Narragansett, RI.

Verdict Media. (2019). *Bluefin SandShark Micro Autonomous Underwater Vehicle.* Retrieved from https://www.naval-technology.com/projects/bluefin-sandshark-micro-autonomous-underwater-vehicle/

# Appendix

| | Large Fin | | Small Fin | |
|---|---|---|---|---|
| **Angle (degrees)** | Lift Force (lb) | Lift Coefficient | Lift Force (lb) | Lift Coefficient |
| 0 | 0 | 0 | 0 | 0 |
| 3 | 0.006 | 0.582 | 0.001 | 0.262 |
| 6 | 0.010 | 0.914 | 0.005 | 1.073 |
| 9 | 0.011 | 0.969 | 0.010 | 2.182 |
| 12 | 0.010 | 0.921 | 0.005 | 1.036 |
| 15 | 0.024 | 2.206 | 0.002 | 0.479 |
| 18 | 0.012 | 1.128 | 0.001 | 0.310 |
| 21 | 0.012 | 1.071 | 0.001 | 0.282 |

Table 1: Collected Data

```
% Jackson Compton
% OCE 311: Fin Analysis Student Project
clc; clear all; close all;                                  % Clear MATLAB
set(0,'defaultAxesFontSize',22,'defaultLineLineWidth'...
    ,3,'DefaultAxesXGrid','on','DefaultAxesYGrid','on',...
    'defaultAxesFontSize',22,'defaultAxesTitleFontSize',2); % Set graph defaults
%% Initial Measurements
rho = 1000;                                                 % Density of water (kg/m^3)
U = 0.12192;                                                % Flow velocity (m/s)
A = [0.00657 0.0026878];                                    % Planform area (m^3)
angle = [0 3 6 9 12 15 18 21];                              % Angle of attack (degrees)
DS = 0.045;                                                 % Sensor moment arm (m)
DLA = 0.135;                                                % Large fin moment arm (m)
DSM = 0.12;                                                 % Small fin moment arm (m)
%% Large Fin
zero = DS*abs(mean(xlsread(['Fin Test Large 0.XLS'],1,...
    'B2:B51')))/DLA;                                        % Calibrate large fin (lb)
for i=1:length(angle)                                       % Loop for angles
    data = xlsread(['Fin Test Large ' num2str(angle(i))...
        '.XLS'],1,'B2:B51');                                % Force readings (lb)
    large_FL(i) = DS*abs(mean(data))/DLA-zero;               % Large fin lift force (lb)
    large_CL(i) = liftcoef(4.44822*large_FL(i),rho,U,A(1)); % Large fin lift coefficient
end                                                         % End loop
%% Small Fin
zero = DS*abs(mean(xlsread(['Fin Test Small 0.XLS'],1,...
    'B2:B51')))/DSM;                                        % Calibrate small fin (lb)
for i=1:length(angle)                                       % Loop for angles
    data = xlsread(['Fin Test Small ' num2str(angle(i))...
        '.XLS'],1,'B2:B51');                                % Force readings (lb)
    small_FL(i) = DS*abs(mean(data))/DSM-zero;               % Small fin lift force (lb)
    small_CL(i) = liftcoef(4.44822*small_FL(i),rho,U,A(2)); % Small fin lift coefficient
end                                                         % End loop
%% Create Figures
figure                                                      % Open figure
    plot(angle,large_FL,'b-o',angle,small_FL,'r-o')         % Plot lift forces
    title('Lift Produced by Foil in 4.8 in/s Water Flow');  % Plot title
    xlabel('Angle of Attack (degrees)');                    % X-axis label
    ylabel('Recorded Lift (lb)');                           % Y-axis label
    set(gca,'FontSize',20);set(gca,'FontWeight','bold');...
        set(gca,'FontName','Times New Roman')               % Set graph format
    set(gca,'tickdir','out')                                % Set tick direction out
    set(gcf,'Color','w')                                    % Set graph background
    legend('Large Fin','Small Fin');                        % Legend
figure                                                      % Open figure
    plot(angle,large_CL,'b-o',angle,small_CL,'r-o')         % Plot lift coefficients
    title('Lift Coefficient vs. Angle of Attack');          % Plot title
    xlabel('Angle of Attack (degrees)');                    % X-axis label
    ylabel('Lift Coeffiecient');                            % Y-axis label
    set(gca,'FontSize',20);set(gca,'FontWeight','bold');...
        set(gca,'FontName','Times New Roman')               % Set graph format
    set(gca,'tickdir','out')                                % Set tick direction out
    set(gcf,'Color','w')                                    % Set graph background
    legend('Large Fin','Small Fin');                        % Legend
%% Create Table
output = [angle',large_FL',large_CL',small_FL',small_CL'];  % Create table
```

Listing 1: MATLAB Script used for Processing Data

```
function [CL] = liftcoef(FL,rho,U,A)
% This function calculates the lift coeffiecient, CL, as a function of the lift
% force, FL, fluid density, rho, flow velocity, U, and the planform area,
% A.
CL = FL/(0.5*rho*U^2*A);
end
```

Listing 2: Lift Coefficient Matlab Function